DOI 10.1002/pmic.200800031 *Proteomics* 2009, *9*, 2064–2075

RESEARCH ARTICLE

NDRG1 is down-regulated in the early apoptotic event induced by camptothecin analogs: The potential role in proteolytic activation of PKCδ and apoptosis

Ying Zheng[1], Li-Shun Wang[1]*, Li Xia[1], Yu-Hui Han[1], Shi-Hua Liao[2], Xiao-Ling Wang[1], Jin-Ke Cheng[1]** and Guo-Qiang Chen[1, 2]*

[1] The Department of Pathophysiology, Key Laboratory of Cell Differentiation and Apoptosis of Chinese Ministry of Education, Shanghai Jiao-Tong University School of Medicine (SJTU-SM), Shanghai, China
[2] Division of Functional Genomics of Cancer, Institute of Health Science, SJTU-SM/Shanghai Institutes of Biological Sciences, Chinese Academy of Sciences, Shanghai, China

We previously reported that NSC606985, a new camptothecin analog, induces apoptosis of acute myeloid leukemic cells, which is triggered by proteolytic activation of protein kinase C delta (PKCδ). Here, we performed quantitative proteomic analysis of NSC606985-treated and untreated leukemic U937 cells with two-dimensional fluorescence difference gel electrophoresis (2-D DIGE) in combination with matrix-assisted laser desorption/ionization time-of-flight/time-of-flight tandem mass spectrometry. Thirty-three proteins were found to be deregulated. Then, we focused on N-myc downstream regulated gene 1 (NDRG1) down-regulated during apoptosis induction. The results demonstrated that the down-regulation of NDRG1 protein but not its mRNA was an early event prior to proteolytic activation of PKCδ in U937 cells under treatments of NSC606985 as well as other camptothecin analogs. With the ectopic expression of NDRG1, the proteolytic activation of PKCδ in NSC606985-treated leukemic cells was delayed and the cells were less sensitive to apoptosis. On the contrary, the suppression of NDRG1 expression by specific small interfering RNA significantly enhanced NSC606985-induced activation of PKCδ and apoptosis of U937 cells. In summary, our study suggests that the down-regulation of NDRG1 is involved in proteolytic activation of PKCδ during apoptosis induction, which would shed new light on the understanding the apoptotic process initiated by camptothecin.

Received: January 12, 2008
Revised: October 27, 2008
Accepted: November 17, 2008

Keywords:
Apoptosis / Camptothecin / N-myc downstream regulated gene 1 / Protein kinase C delta

Correspondence: Dr. Guo-Qiang Chen, The Department of Pathophysiology, Key Laboratory of Cell Differentiation and Apoptosis of Chinese Ministry of Education, Shanghai Jiao-Tong University School of Medicine, No 280, Chong-Qing South Road, Shanghai 200025, China
E-mail: chengq@shsmu.edu.cn
Fax: +86-21-6415-4900

Abbreviations: **AML**, acute myeloid leukemia; **NDRG1**, N-myc downstream regulated gene 1; **PARP**, poly(ADP [adenosine diphosphate]–ribose) polymerase; **PKCδ**, protein kinase C delta; **siRNA**, small interfering RNA

1 Introduction

Apoptosis is a genetically determined cell suicidal program that removes unwanted, redundant and damaged cells, and is required for the maintenance of tissue homeostasis in multicellular organisms [1]. Defects in the apoptotic program have been associated with many diseases such as can-

* These authors contributed equally to this work.
** Additional corresponding author: Dr. Jin-Ke Cheng; E-mail: jkcheng@shsmu.edu.cn

cer [2]. Many chemotherapeutic agents are known to induce apoptotic cell death, and deregulation in apoptosis results in treatment failure [3]. It is believed that DNA damage caused by chemotherapeutic drugs induces mitochondria to release cytochrome c, facilitating the interaction of Apaf-1 with initiators upstream caspase-9 and initiating a downstream caspase cascade, especially caspase-3 [4]. However, the initial signaling triggering apoptosis may vary significantly, which appears to depend on the apoptotic stimulus as well as the cellular context [4, 5]. The signaling pathway that links DNA damage to apoptotic cell death is a subject of intense investigation.

Protein kinase C (PKC) represents a family of phospholipid-dependent serine/threonine protein kinases. It includes at least 11 isozymes that have been categorized into three groups: conventional PKCs (α, βI, βII and γ), novel PKCs (δ, ε, η and θ), and atypical PKCs (ζ and λ/τ). These PKC isozymes have long been known for their roles in the growth factor signal transduction pathways [6]. For example, activation of stably overexpressed PKCδ upon treatment with phorbol 12-myristate 13-acetate markedly induced growth arrest with accumulation in G_2/M cells of several lines of CHO cells [7]. In 1995, Emoto *et al.* [8] identified a novel function of PKCδ in the apoptotic signaling pathway, because the death stimulus, such as ionizing radiation, results in proteolytic activation of PKCδ, which can be inhibited by caspase inhibitors and anti-apoptotic proteins, such as Bcl-2 or Bcl-xL. From then on, proteolytic activation of PKCδ has been associated with apoptosis induced by various DNA-damaging agents, including UV radiation, ionizing radiation, cisplatin, etoposide, cytosine arabinoside, mitomycin C, and doxorubicin [9–11].

Later, PKCδ was demonstrated to be a substrate for caspase-3, which cleaves PKCδ at the $DMQD^{330}N$ site in its hinge region, generating a 41-kDa C-terminal catalytic fragment. The separation of the autoinhibitory regulatory domain from the catalytic domain results in activation of PKCδ [8]. Therefore, PKCδ was believed to act downstream of the executioner caspase-3, and proteolytic activation of PKCδ is accepted as apoptosis promotion factor, as widely reviewed [12, 13]. Nevertheless, it was also reported that PKCδ activation is essential for apoptosis induction following exposure of cells to several DNA damaging agents such as etoposide [11], *cis*-diamminedichloroplatinum (cDDP) [14], and camptothecin ester derivative NSC606985 [15]. Rottlerin, an inhibitor of PKCδ, inhibited cisplatin and NSC606985-induced proteolytic processing of PKCδ as well as activation of caspase-3. Furthermore, overexpression of the catalytic fragment of PKCδ was sufficient to induce apoptosis, as evidenced by poly(ADP [adenosine diphosphate]–ribose) polymerase (PARP) cleavage [16]. These observations strongly suggested that activation of PKCδ occurs early in the apoptotic pathway, and that PKCδ may act upstream of caspase-3 to regulate its activation [11, 14, 17, 18]. In this sense, there may be a feedback loop between PKCδ and caspase-3. The feedback loop amplifies caspase-3-mediated activation of PKCδ. However, little work was done on how DNA damage-related apoptosis stimulus directly proteolytically activates PKCδ prior to caspase-3 activation. To find the proteins that are deregulated ahead of and thus possibly involved in proteolytic activation of PKCδ, we performed quantitative proteomic analysis (2-D DIGE) of NSC606985-treated acute myeloid leukemia (AML) cell line U937 cells at 0, 12, and 18 h, the time points before the cleavage activation of PKCδ, and 33 proteins were identified to be changed. After some preliminary experiments, we focused on N-myc downstream regulated gene 1 (NDRG1), which is down-regulated during apoptosis induction. Our results demonstrate that the down-regulation of NDRG1 protein is an early event prior to proteolytic activation of PKCδ in U937 cells under NSC606985 as well as other camptothecin analog treatment. The ectopic expression of NDRG1 delays the proteolytic activation of PKCδ in NSC606985-treated leukemic U937 cells and makes the cells less sensitive to apoptosis. On the contrary, the suppression of NDRG1 expression by specific small interfering RNA (siRNA) significantly enhances NSC606985-induced activation of PKCδ and apoptosis of U937 cells. These results would provide clues for understanding the apoptotic process initiated by camptothecin.

2 Materials and methods

2.1 Cell culture and treatment

AML cell line U937 (from Cell Bank of Shanghai Institutes of Biological Sciences, Shanghai, China) was cultured in RPMI-1640 medium (Sigma, St Louis, MI) supplemented with 10% fetal calf serum (Gibco BRL, Gaithersburg, MD) in a 5% CO_2/95% air at 37°C. The cells, which were seeded at 4×10^5 cells/mL, were treated with or without the indicated concentrations of NSC606985 (generous gift from National Cancer Institute Anticancer Drug Screen standard agent database), topotecan, irinotecan (purchased from Shanghai Biocompounds ChemLa Co), and doxorubicin (BIOMOL, Plymouth, PA).

2.2 Protein preparation

The treated and untreated U937 cells were counted and harvested by centrifugation, washed twice with Tris-buffered sucrose (10 mM Tris-Base, 250 mM sucrose pH 7.0), and dissolved in lysis buffer containing 7 M urea, 2 M thiourea, 30 mM Tris-Base, 4% m/v CHAPS, 0.2% Bio-lyte 3/10 ampholyte (Bio-Rad, Hercules, CA). Following incubation for 1 h at room temperature to allow solubilization, the samples were centrifuged at $40\,000 \times g$ for 1 h at 4°C to eliminate potentially insolubilized debris. The supernatant was used immediately or divided into aliquots and stored at –80°C for subsequent analysis. Protein concentration was determined using the Bio-Rad RC DC protein assay kit (Bio-Rad). The concentration of the protein lysate was adjusted to 5 mg/mL and the pH to 8.5.

2.3 DIGE labeling

Samples were labeled with N-hydroxy succinimidyl ester derivatives of the cyanine dyes Cy2, Cy3 and Cy5 (GE Healthcare, UK) following a standard protocol [19]. Shortly, 50 μg of NSC606985 treated or untreated cell lysate was minimally labeled with 400 pmol of either Cy3 or Cy5 for comparison on the same 2-D gel. Labeling reactions were performed on ice in the dark for 30 min and then quenched with a 50-fold molar excess of free lysine for 10 min on ice. A pool of all samples was also prepared and labeled with Cy2, which was used as an internal standard on all gels to aid image matching and cross-gel statistical analysis.

2.4 2-DE

The soluble protein fraction was analyzed by 2-DE as previously described [20]. Briefly, IEF was performed in 17-cm IPG (pH 3–10) nonlinear strips (Bio-Rad) with 150 μg protein load/strip until 80 kVh were reached. Once the IEF was completed, the IPG strips were equilibrated for 30 min with 50 mM Tris-HCl, pH 8.8, 6 M urea, 30% glycerol, 2% SDS, followed by reduction with 1% of DTT and alkylation with 4% iodoacetamide. The second dimension separations were carried out on 12.5% SDS-PAGE, and gels were run at 16 mA/gel for 30 min, and then 24 mA/gel until the dye run to the bottom of the gels. Three replicas from each sample were made following this procedure.

2.5 Gel image and image analysis

All the images were collected on a Typhoon TRIO+ scanner (GE Healthcare, Freiburg, Germany) with a resolution of 100 μm. Spot detection was performed on the gel images using the DeCyder software (Version 6.5) module DIA (version 6.5.14) setting the target spot number to 2500. All six gels were added to the appropriate workspace and group and matched to a master gel sequentially using the DeCyder module BVA (version 6.5.14). The fluorescent signal of a spot was background-corrected and normalized by the DeCyder software (version 6.5). Before the matching process was started, up to 200 landmarks have been defined all over the gel followed by careful manual rematching of wrongly matched spots or unmatched spots. Subsequently, the matching process was started followed by reviewing all matches that were classified by the algorithm as level 1 match (automatic matches with high confidence) and confirming all correct matches. The cycle of matching, reviewing and confirming the matches was repeated until no new level 1 matches were found. Using the DeCyder module XML Toolbox, the spot raw data especially the volume ratio for each gel were exported from DeCyder and analyzed using SPSS 13.0 (SPSS, Chicago, IL). Protein spots with significant changes (paired *t*-test, $p < 0.05$) in a consistent direction (increase or decrease) were selected for further identification.

2.6 In-gel digestion and MS

The protein spots were cut out of 2-D gels using Gelpix Spot-Excision Robot (Genetix, Hampshire, UK), transferred into 96-well plate, and destained with equal volume of 30 mM potassium ferricyanide and 100 mM sodium thiosulfate at room temperature, followed by washing with Milli-Q water, 25 mM ammonium bicarbonate/50% ACN and 100% ACN. Then the gel pieces were dried in a vacuum and the proteins were digested overnight in 10 μL of trypsin (7 ng/μL, Trypsin Gold, MS grade, Promega, Madison, WI) in 25 mM ammonium bicarbonate at 37°C. The reaction was terminated with 1 μL 1% TFA and the peptide fragments were enriched and desalted with ZipTip pipette (Millipore, Billerica, BA) tips according to the manufacture.

Tryptic peptides were lyophilized and resuspended in 1 μL matrix solution containing 5 mg/mL CHCA prepared in 50% ACN/0.1% TFA. The samples were spotted onto the MALDI sample target plate and analyzed with MALDI-TOF-TOF mass spectrometer (4700 Proteomics Analyzer, Applied Biosystem, Foster City, CA) as previously described [20]. Protein identification was processed and analyzed by searching the Swiss-Prot protein database using the MASCOT search engine of Matrix Science that integrated in the Global Protein Server Workstation. The mass tolerance, the most important parameter, was limited to 50 ppm. The results from both the MS and MS/MS spectra were accepted as a good identification when the GPS score confidence was higher than 95%.

2.7 Establishment of U937^{NDRG1} stable transformants

U937T cells (kindly provided by Dr. D. G. Tenen of Harvard Institutes of Medicine, Harvard Medical School, Boston, MA) with stably transfected pTRE-tTA, a tetracycline responsive transcription activator (tTA) whose expression is under the control of tetracycline [21]. Human full-length NDRG1 cDNA, which was amplified from pBI-EGFP-NDRG1 (donated by Dr. P. Liang, Vanderbilt University Medical Center, Nashville, TN) [22], was subcloned into the MluI and EcoRV sites of pTRE2hyg expression vector (BD clontech, Palo Alto, CA) to form pTRE2hyg-NDRG1. The sequence of the cDNA insert of the plasmid was confirmed by sequencing. To generate U937^{NDRG1} stable transformant, 1×10^7 of U937T cells were washed in RPMI 1640-medium and resuspended in 0.2 mL of Iscove's Modified Dulbecco's medium (IMDM) without FBS. Twenty micrograms of pTRE2hyg-NDRG1 or, as a control, empty plasmid pTRE2hyg in 20 μL double-distilled H_2O, was transferred to electroporation cuvette with a 0.4-cm gap (Bio-Rad). Electroporation was performed at 170 V and 960 μF using a Gene-Pulser II (Bio-Rad). The samples were then transferred to complete RPMI-1640 medium. Twenty-four hours later, 1 μg/mL of tetracycline, 0.5 μg/mL of puromycin and 0.5 mg/mL hygromycin B (BD clontech) were added and cells were continued to incubate at 37°C in 5% CO_2. Positive polyclonal population

(pool) was identified based on the induction of NDRG1 expression following tetracycline withdrawal and was named U937^{NDRG1}. As a control, empty plasmid-transfected cell line was called U937^{empty}. U937^{NDRG1} and U937^{empty} cells were maintained in RPMI-1640 medium supplemented with 10% FBS, 1 μg tetracycline, 0.5 μg puromycin and 0.5 mg hygromycin B/mL.

2.8 SiRNA stable expression

The mammalian expression vector, pSilencer 3.1-H1 neo (Ambion, Austin, Texas) was used for expression of siRNA in U937 cells. SiRNA to NDRG1 were designed following the procedure from Ambion (Austin, Texas). Its target sequence was 5'-GGA GTC CTT CAA CAG TTT G-3', as described [23]. For the target sequence, we designed complementary 70-mer oligonucleotides with 5' single-stranded overhangs for ligation into the pSilencer 3.1-H1 neo vector. The oligonucleotides encoded 19-mer hairpin sequences specific to NDRG1 mRNA target, a loop sequence separating the two complementary domains, and a polythymidine tract to terminate transcription. The sequence was synthesized and inserted into the pSilencer 3.1-H1 neo vector according to manufacturer's instructions (Ambion). The specific siRNA or negative control siRNA (Ambion) was transfected into U937 cells by Nucleofector™ Solution (Amaxa, Gaithersburg, MD) according to manufacturer's instructions. Twenty-four hours after transfection, 1 mg/mL G418 was added to the medium to select for the stably transfected cells.

2.9 Real-time quantitative RT-PCR

Total cellular mRNA from cell lines were extracted by TRIzol reagent (Invitrogen, Carlsbad, CA) and were treated with RNase-free DNase (Promega, Madison, WI). Then, reverse transcription (RT) was performed by TaKaRa RNA PCR kit (Takara, Dalian, China) following manufacturer's protocol. For real-time quantitative RT-PCR, the following specific oligonucleotide primers were used, respectively, for NDRG1 (forward primer CGCCAGCACATTGTGAATGAC and reverse primer TTTGAGTTGCACT CCACCACG), with β-actin (forward primer CATCCTCACCCTGAAG TACCC and reverse primer AGCCTGGATAGCAACGTA CATG) as internal control. Real-time RT-PCR was performed and data were analyzed according to a previous report [24].

2.10 Cycloheximide inhibition test

U937 cells were treated with 10 μg/mL cycloheximide (CHX, Sigma-Aldrich, St Louis, MO) combined with or without 50 nM NSC606985 for the indicated times. NDRG1 protein was determined by the Western blot using β-tubulin as loading control.

2.11 Western blot

Cells were harvested and lysed with ice-cold lysis buffer (62.5 mM Tris-HCl, pH 6.8, 100 mM DTT, 2% w/v SDS, 10% glycerol, 0.01% w/v bromophenol blue). After centrifugation at 20 000 $\times g$ for 10 min at 4°C, proteins in the supernatants were quantified and separated by 10% or 12% SDS-PAGE, and transferred to NC membrane (Amersham Bioscience, Buckinghamshire, UK). After blocking with 5% nonfat milk in PBS, membranes were immunoblotted with antibodies directed against cap43 (NDRG1) (1:1000, ZYMED, South San Francisco, CA), PKCδ (1:5000, C-20; Santa Cruz Biotech, Santa Cruz, CA), cleave caspase-3 (1:1000; Cell Signaling, Beverly, MA), and PARP (1:1000, F2, Santa Cruz Biotech), followed by HRP-linked secondary antibodies (Cell Signaling). Mouse anti-β-tubulin (Sigma) was used as an internal control. The signals were detected by SuperSignal West Pico Chemiluminescent Substrate kit (Pierce, Rockford, IL) according to manufacturer's instructions. All experiments were repeated three times with the similar results.

2.12 Flow cytometric assay for annexin-V

Annexin-V assay was performed on a flow cytometry (Beckman Coulter) according to instructions provided by the BD PharMingen Annexin-V-FITC Apoptosis Detection kit (BD, San Diego, CA). Approximately 2×10^5 cells were rinsed with 1 × Binding Buffer and cells were then resuspended in 100 μL of 1 × Binding Buffer. Then, 5 μL Annexin V-FITC and PI were added, respectively. After 15 min of incubation in the dark at room temperature, apoptosis was evaluated by flow cytometry.

2.13 Statistical analysis

The values were expressed as mean ± SD. The paired *t*-test was used for statistical analysis between two groups. Significant level was set at $p < 0.05$.

3 Results

3.1 NSC606985-modulated protein expression profiles prior to PKCδ activation in U937 cells

Consistent with our previous report [15], under 50 nM NSC606985 treatment for 36 h, U937 cells underwent apoptosis, as assessed by proteolytic activation of caspase-3 and the cleaved PARP (Fig. 1A) as well as annexin-V assay (data not shown). Prior to caspase-3 activation, PKCδ was proteolytically activated with the appearance of its catalytic fragment of 41 kDa, which could be clearly observed at 21 h after NSC606985 treatment. Notably, the full size PKCδ band is usually not reduced in apoptotic cells although the PKCδ cleavage product appears at high levels in most cases. We speculated that it might be due to higher basal level of PKCδ

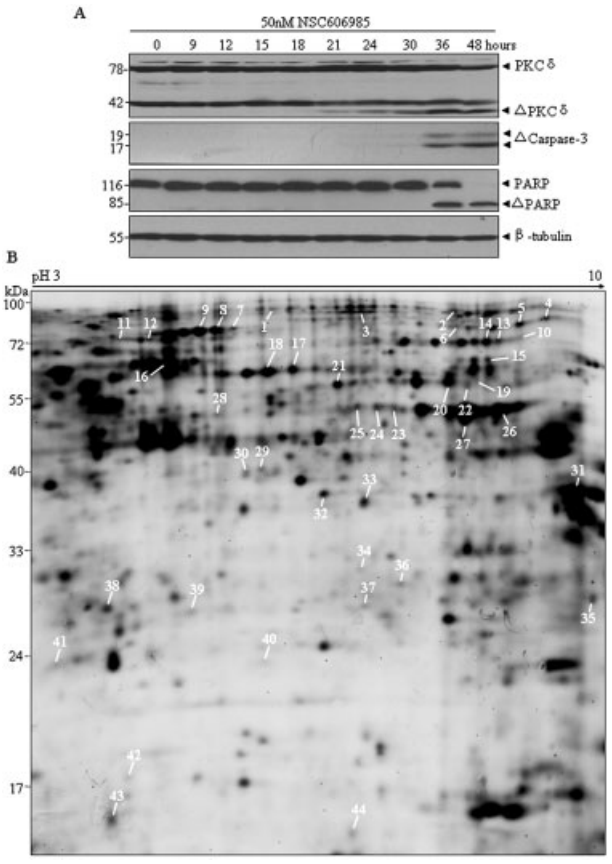

Figure 1. Representative 2-D DIGE image of U937 cells treated by NSC606985. (A) U937 cells were incubated with 50 nM NSC606985 for 0, 9, 12, 15, 18, 21, 24, 30, 36 and 48 h. Western blot analysis of proteolytic activation of PKCδ, and Caspase 3 and PARP cleavage served as apoptotic markers. Equal loading of protein was confirmed using anti-β-tubulin. (B) Protein expression profiling of NSC606985-treated and untreated U937 cells were compared by 2-D DIGE. The first dimension was performed by IEF on pH 3–10 (17-cm nonlinear) IPG strips, followed by the second dimension on a 12.5% gel. The differences of expression were analyzed using DeCyder software. The differentially expressed spots were indicated with serial numbers. They were subsequently excised and identified by MALDI-TOF/TOF mass spectrometer. The complete information is shown in Table 1.

in U937 cells and/or higher sensitivity of anti-PKCδ antibody used [15, 25]. To provide some clues for molecular mechanisms of the proteolytic activation of PKCδ induced by NSC606985, U937 cells with 50 nM of NSC606985 treatment for 0 and 12 or 18 h, time points at which PKCδ activation was undetectable, were extracted and comparative proteomic analysis was performed by 2-D DIGE. All gels were scanned with Typhoon TRIO+ scanner. Figure 1B shows a representative 2-D DIGE gel image of U937 cells with and without NSC606985 treatment for 12 h. Spot detection and spot differential analysis were performed using the DeCyder software module DIA and BVA. Totally, 44 spots were found to be modulated to more than 1.3-folds after 12 and/or 18 h of NSC606985 treatment (Fig. 1B). Those deregulated spots were excised from the gels and digested with trypsin enzyme for MS analysis. As an example, spot 28 was found to be down-regulated after NSC606985 treatment for 12 h (Fig. 2A) and it was identified as NDRG1 by MALDI-TOF/TOF PMF and/or MS-MS analysis (Figs. 2B, C). Totally, 39 spots were identified, consisting of 33 unique proteins (Table 1, Fig. 1B). They are involved in cytoskeleton and molecular chaperoning, DNA and RNA processing, glycolysis and energy metabolism, cell proliferation and apoptosis, and others, respectively.

3.2 Decrease of NDRG1 protein is an early event in multiple chemotherapeutic drugs-treated cells

In the next phase of analysis, U937 cells were treated with 50 nM of NSC606985, and NDRG1 and PKCδ proteins were dynamically measured by Western blot. As shown in the left panel of Fig. 3A, NDRG1 protein was reduced, which began to appear at 6 h and became more and more significant later, while proteolytic activation of PKCδ was seen at 24 h after NSC606985 treatment. Furthermore, 1 μM doxorubicin (right panel of Fig. 3A), 100 nM topotecan (right panel of Fig.3B) or 5 μM irinoticon (right panel of Fig. 3B) was also applied to U937 cells for the different times. Like seen in NSC606985-treated cells, these three chemotherapeutic drugs also decreased NDRG1 protein before the proteolytic cleavage of PKCδ and the activation of caspases-3, indicating that the down-regulation of NDRG1 protein prior to PKCδ activation is common to all DNA-damage agents. To exclude the possibility that low levels of active PKCδ and caspases-3, which might not be detectable by immunoblot, may suffice to cause degradation of NDRG1, U937 cells were pre-incubated with the PKCδ-specific inhibitor rottlerin or caspase-3 inhibitor Z-DEVD-fmk for 1 h before the addition of 50 nM NSC606985. The results demonstrated that the pretreatment of either rottlerin or Z-DEVD-fmk failed to significantly rescue the down-regulation of NDRG1 induced by NSC606985, although proteolytic cleavage of PKCδ or activation of caspase-3 could be effectively inhibited by rottlerin or Z-DEVD-fmk (Figs. 3C, D). These results indicated that NSC606985-induced NDRG1 down-regulation was an early event upstream to the PKCδ activation and activated PKCδ or caspase-3 had little effect on NDRG1 expression in U937 cells.

3.3 Down-regulation of NDRG1 protein during NSC606985 treatment is not associated with its transcription

Although the down-regulation of NDRG1 protein rapidly occurred, we still sought to examine whether NSC606985 regulates transcriptional expression of NDRG1 gene by real-time quantitative RT-PCR. The results demonstrated that NSC606985 only induced a rapid and transitory reduction of NDRG1 mRNA, which was recovered to the basal level at 12 and 24 h and later increased slightly (Figs. 4A, B). Then, we

Table 1. The deregulated proteins of NSC606985 induced apoptotic U937 cells[a)]

Classification/ gene symbol[b)]	Protein name	Spot no.	Mean-fold		p/ theor./ exptl.[e)]	MW theor./ exptl.	PMF			MS/MS	
			12h/0h (n = 3)[c)]	18h/0h (n = 3)[d)]			Pep.[f)]	Cov[g)]	Sco.[h)]	Pep.	Sco.
Cytoskeleton and molecular chaperone											
GRP75	75KDa glucose regulated protein	7	–1.2 ± 0.1	–1.5 ± 0.2	5.9/5.8	73.9/73.1	22	37	145	2	79
GRP75	75KDa glucose regulated protein	8	–1.2 ± 0.1	–1.4 ± 0.1	5.9/5.6	73.9/73.1	45	30	248	2	79
GRP75	75KDa glucose regulated protein	9	–1.1 ± 0.1	–1.3 ± 0.1	5.9/5.4	73.9/73.1	13	24	69	2	45
HSP7C	Heat shock cognate 71 kDa protein	9	–1.1 ± 0.1	–1.3 ± 0.1	5.9/5.4	70.9/73.1	19	39	134	2	131
LMNB1	LaminB1	11	–1.1 ± 0.1	–1.3 ± 0.2	5.1/5.0	66.7/60.7	25	40	167	4	102
PLSL	Plastin2	12	–1.3 ± 0.1	–1.2 ± 0.1	5.2/5.2	70.8/60.4	29	44	209	2	44
CH60	60 kDa heat shock protein, mitochondrial precursor (Hsp60)	16	–1.4 ± 0.1	–1.6 ± 0.1	5.7/5.3	61.2/62.2	18	35	125	3	228
PDIA3	Disulfide isomerase ER60 (ERp60)	17	–1.3 ± 0.1	–1.3 ± 0.2	6.0/6.1	57.1/61.5	33	60	309	3	230
PDIA3	Disulfide isomerase ER60 (ERp60)	18	–1.2 ± 0.1	–1.3 ± 0.1	6.0/6.0	57.1/61.5	20	37	122		
TCPB	T-complex protein 1, beta subunit	21	–1.1 ± 0.1	–1.4 ± 0.2	6.0/6.2	57.7/57.6	38	74	358	3	167
ERP29	Endoplasmic reticulum protein ERp29 precursor	34	1.4 ± 0.2	1.2 ± 0.2	6.8/6.2	29.0/31.5	19	63	140	4	241
HMGB1	High mobility group protein B1	37	–1.2 ± 0.1	–1.6 ± 0.2	5.6/6.2	25.0/28.2	15	51	113	2	87
HSPB1	Heat shock 27 kDa protein	39	1.6 ± 0.4	1.8 ± 0.2	5.3/5.3	42.1/28.5	14	52	124	3	171
DNA and RNA processing											
DDX5	Probable ATPdependent RNA helicase DDX5	10	–1.2 ± 0.1	–1.5 ± 0.2	9.1/7.1	69.6/72.1	14	23	66	2	22
HNRPL	Heterogeneous nuclear ribonucleoprotein L	13	–1.2 ± 0.1	–1.4 ± 0.2	6.7/7.0	60.7/65.8	18	29	109	1	9
HNRPL	Heterogeneous nuclear ribonucleoprotein L	14	–1.2 ± 0.1	–1.4 ± 0.1	6.7/7.0	60.7/65.8	24	40	177	4	55
CPSF5	Cleavage and polyadenylation specificity factor subunit 5	35	1.2 ± 0.1	1.3 ± 0.1	8.9/9.9	26.3/29.3	17	55	161	4	139
ROA1	Heterogeneous nuclear ribonucleoprotein A1	44	1.2 ± 0.1	1.3 ± 0.2	9.3/6.3	38.9/15.2	13	29	96	5	100
Glycolysis and energy metabolism											
KPYM	Pyruvate kinase isozymes M1/M2	19	–1.3 ± 0.2	–1.6 ± 0.1	8.0/6.8	58.5/57.6	15	35	99		
KPYM	Pyruvate kinase, isozymes M1/M2	20	–1.3 ± 0.2	–1.5 ± 0.2	8.0/6.6	58.5/57.5	36	63	310	2	55
ENOA	Alphaenolase	23	–1.3 ± 0.1	–1.3 ± 0.1	7.0/6.4	47.4/53.1	15	37	97	3	98
ENOA	Alphaenolase	24	–1.1 ± 0.1	–1.4 ± 0.1	7.0/6.3	47.4/53.1	16	42	112	2	87
ENOA	Alphaenolase	26	–1.3 ± 0.2	–1.7 ± 0.2	7.0/7.2	47.4/53.3	18	53	140	2	150
ENOA	Alphaenolase	27	–1.2 ± 0.2	–1.3 ± 0.2	7.0/6.7	47.4/53.3	13	30	68		
ENOA	Alphaenolase	29	1.4 ± 0.3	1.5 ± 0.2	7.0/5.9	47.4/40.0	12	32	73	1	12
G3P2	Glyceraldehyde-3-phosphate dehydrogenase, liver	31	–1.4 ± 0.1	–1.5 ± 0.2	8.6/9.8	36.1/38.2	18	52	140	2	149
GALK1	Galactokinase	32	1.2 ± 0.1	1.3 ± 0.1	6.0/6.2	42.7/38.2	17	46	144	4	106
TALDO	Transaldolase	33	1.4 ± 0.1	1.5 ± 0.2	6.4/6.3	37.7/37.2	17	35	107	2	35
PGAM1	Phosphoglycerate mutase 1	36	1.1 ± 0.1	1.3 ± 0.1	6.7/6.4	28.9/29.1	15	58	123	2	11
Cell proliferation and apoptosis											
PA2G4	Proliferation-associated protein 2G4	22	–1.2 ± 0.2	–1.6 ± 0.1	6.1/6.2	44.1/52.8	25	54	153	5	171
NDRG1	Protein NDRG1	28	–1.3 ± 0.1	–1.3 ± 0.1	5.5/5.7	43.3/51.6	15	37	73	1	44
AN32A	Acidic leucine-rich nuclear phosphoprotein 32 family member A	41	1.5 ± 0.4	1.2 ± 0.1	4.0/3.8	28.7/23.7	9	30	78	4	174
Others											
IMMT	Mitochondrial inner membrane protein (Mitofilin) (p87/89)	1	–1.2 ± 0.1	–1.6 ± 0.1	6.1/6.0	84.0/99.6	19	29	124	2	12
ZYX	Zyxin	3	–1.2 ± 0.1	–1.3 ± 0.1	6.2/6.3	62.4/98.6	14	31	115	3	40

Table 1. Continued

Classification/ gene symbol[b)]	Protein name	Spot no.	Mean-fold		p*I* theor./ exptl.[e)]	MW theor./ exptl.	PMF			MS/MS	
			12h/0h (n = 3)[c)]	18h/0h (n = 3)[d)]			Pep.[f)]	Cov[g)]	Sco.[h)]	Pep.	Sco.
FUBP1	Far upstream element binding protein 1	5	–1.1 ± 0.1	–1.3 ± 0.1	7.2/7.1	67.7/72.6	21	33	129	4	63
CATA	Catalase	15	–1.2 ± 0.2	–1.5 ± 0.2	6.9/7.0	60.0/62.3	21	47	188	3	126
NAMPT	Nicotinamide phosphoribosyl-transferase	19	–1.3 ± 0.2	–1.6 ± 0.1	6.7/6.8	55.8/57.6	10	25	62		
DHE3	Glutamate dehydrogenase 1, mitochondrial precursor	22	–1.3 ± 0.2	–1.5 ± 0.1	7.7/6.7	61.7/57.5	24	42	171	1	26
CAPG	Macrophage capping protein	30	1.5 ± 0.2	1.6 ± 0.5	5.9/5.9	38.8/39.8	10	28	52	2	56
MDHM	Malate dehydrogenase, mitochondrial precursor	31	–1.4 ± 0.1	–1.5 ± 0.2	8.9/9.8	36.0/38.2	11	48	93	2	65
PSA3	Proteasome subunit alpha type3	38	1.4 ± 0.1	1.3 ± 0.1	5.2/5.1	28.6/28.8	12	40	89	1	5
H2B1M	Histone H2B type 1M	43	1.6 ± 0.5	1.9 ± 0.4	10.3/5.1	13.8/15.5	12	53	65	1	31

a) U937 cells were treated with 50 nM NSC606985 for 0, 12, and 18 h, and the proteins were extracted and separated by 2-D DIGE. The deregulated spots were numbered respectively according to their locations on the 2-DE maps. They are classified into different sections according to their primary functions. DeCyder software-aided spot intensity ratio of 12 and 18 *vs.* 0 h, respectively, as well as the experimental isoelectric point and molecular weight are provided for each identified protein. Theoretical p*I* and molecular weights are derived from the amino-acid sequences in Swiss-Prot.
b) Classification in Swiss-Prot database.
c) NSC606985 treatment 12 *vs.* 0 h.
d) NSC606985 treatment 18 *vs.* 0 h.
e) Theoretical *vs.* experimental.
f) Peptide counts matched in MS analysis.
g) Coverage by the matched peptides.
h) The scores of identified proteins by MASCOT analysis.

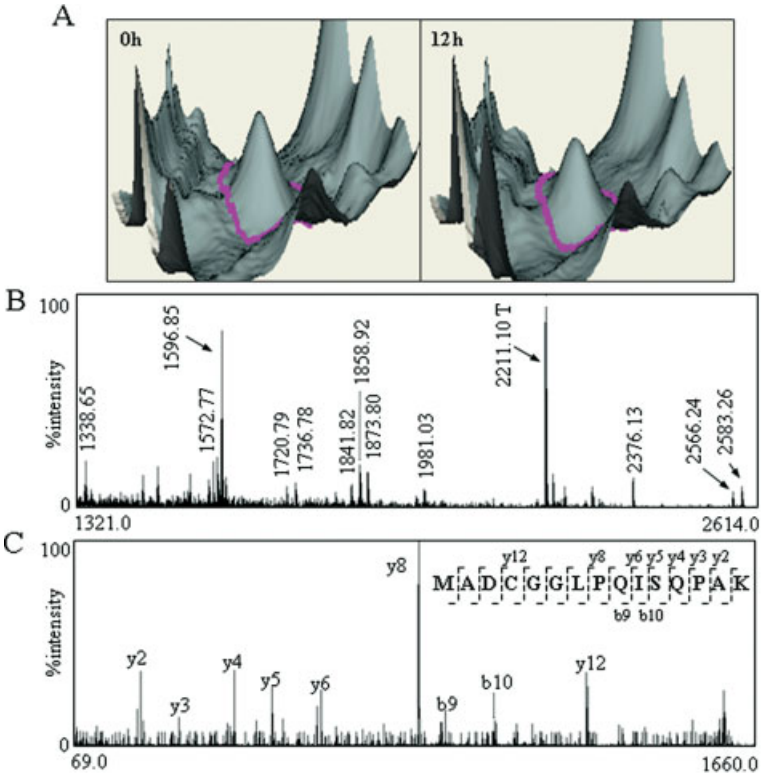

Figure 2. DIGE of NDRG1 and its MS analysis. (A) Images were generated using the BVA module of DeCyder software and visually 3-D images show the abundance levels of spot 28 (indicated by the red circles) were down-regulated in U937 cells treated with 50 nM NSC606985 for 12 h compared to those untreated. (B) PMF of tryptic peptides from spot 28. "T" indicates trypsin autolytic peptides for internal calibration and arrows indicate peaks matched NDRG1. The matched peptides occupy 37% sequence coverage and obtain 73 score. (C) Fragmentation spectrum for ion 1596.85. The y-ions, b-ions as well as internal fragment ions and immonium ions are denoted in the spectrum. The *m/z* 1596.85 is one of the abundant peaks selected for MS/MS acquisition. The identified sequence is MADCGGLPQISQPAK interpreted as y series and b series ions, which are indicated in the top right corner.

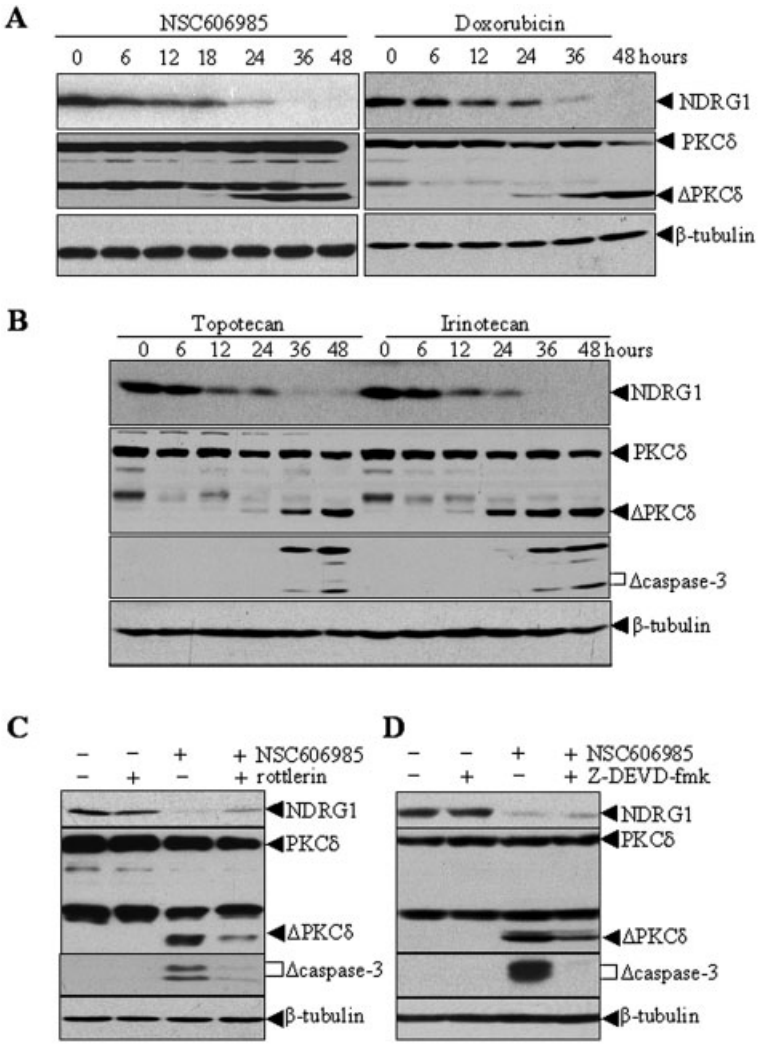

Figure 3. Down-regulation of NDRG1 appears prior to proteolytic activation of PKCδ. (A, B) The dynamic expression of NDRG1 and the proteolytic activation of PKCδ were analyzed in the 50 nM NSC606985 (left, A), 1 μM doxorubicin (right, A), 100 nM topotecan (left, B) or 5 μM irinoticon (right, B)-treated U937 cells at hours as indicated. (C, D) After pre-incubation for 1 h in the presence or absence of 3 μM rottlerin (C) or 50 μM Z-DEVD-fmk (D), U937 cells were treated with 50 nM NSC606985 for 36 h. The indicated proteins were detected by western blots probed with specific antibodies with β-tubulin as equal loading control. All experiments were repeated for three times with the same results.

tested whether NSC606985 impinges on the degradation of NDRG1 protein by cycloheximide (CHX) inhibition test. For this purpose, U937 cells were treated dynamically with 10 μg/mL CHX (an inhibitor of protein synthesis) alone or combined with NSC606985. As shown in Fig. 4C, the half-life of NDRG1 did not change significantly under these treatments. Notably, CHX treatment also cleaved PKCδ and induced caspase-3 activation in this experimental system (Fig. 4C).

3.4 Inducible NDRG1 expression delays proteolytic activation of PKCδ and inhibits apoptosis induction

Previously, we concluded that the proteolytic activation of PKCδ plays a key role in NSC606985-induced leukemic cell apoptosis [15]. To investigate the potential influence of NDRG1 expression on the proteolytic activation of PKCδ, we generated inducible NDRG1-expressing U937T cell line by a Tet-Off gene expression system. NDRG1 cDNA was inserted into a tetracycline-responsive expression vector (plasmid pTRE2hyg) to form pTRE2hyg-NDRG1. Then, pTRE2hyg-NDRG1 or empty plasmid pTRE2hyg was transfected into the U937T cells with stably transfected pTRE-tTA, a tetracycline responsive transcription activator (tTA) whose expression is under the control of tetracycline [21]. In principle, while cultured in medium with tetracycline, the expression of tTA and NDRG1 should be extremely low. On the contrary, in the absence of tetracycline, tTA activates its own promoter to produce more tTA, the latter subsequently activating NDRG1 expression. U937T cells stably transfected with empty vector and pTRE2hyg-NDRG1 were respectively named $U937^{empty}$ and $U937^{NDRG1}$ cells. When grown in tetracycline-free medium for 6 days, $U937^{NDRG1}$, but not $U937^{empty}$, cells presented higher NDRG1 expression (Fig. 5A). Then, these cells were treated with a higher concentration (200 nM) of NSC606985 for the different times. Unlike $U937^{empty}$ cells or $U937^{NDRG1}$ cells in tetracycline-

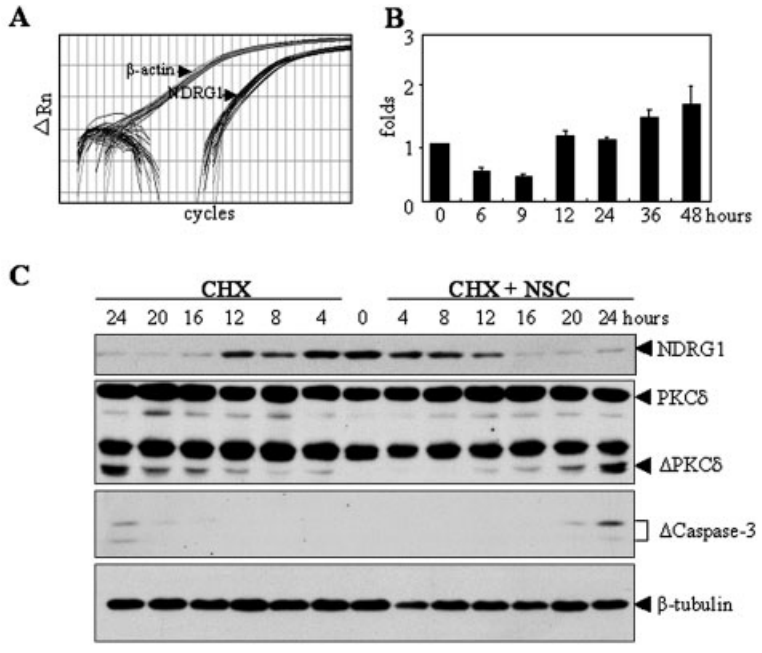

Figure 4. The expression of NDRG1 mRNA and its protein half-life under NSC606985 treatment. (A) Typical amplification plots for NDRG1 and β-actin showing how their relative expression levels can be assayed by real-time RT-PCR. (B) The panel shows the NDRG1 mRNA level detected by real-time quantitative PCR under NSC606985 treatment for times as indicated. Altered folds of NDRG1 mRNA against untreated cells are shown as means ± SD in three independent experiments. (C) U937 cells were treated with 50 nM NSC606985 or combined with 10 μg/mL cycloheximide (CHX) for the indicated hours. The indicated proteins were detected by western blots probed with specific antibodies with β-tubulin as equal loading control. All experiments were repeated for three times with the same results.

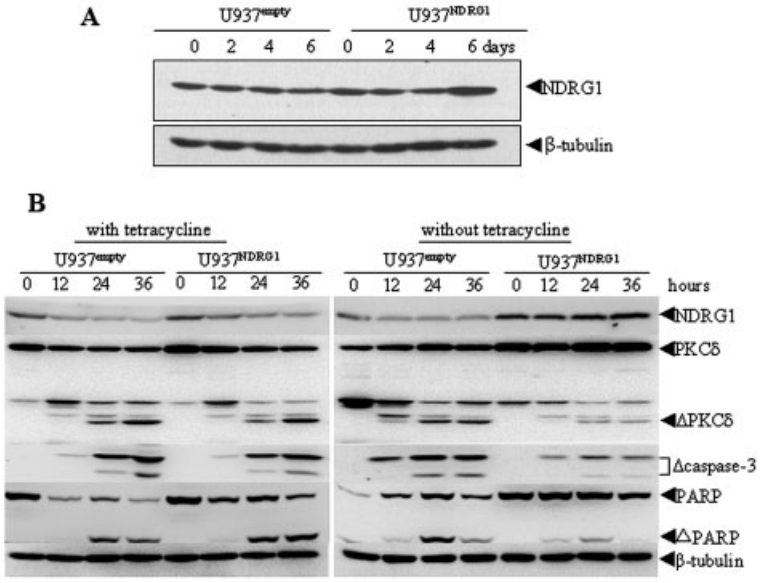

Figure 5. Inducible NDRG1 delays proteolytic activation of PKCδ. (A) U937T cells stably transfected with pTRE2hyg and pTRE2hyg-NDRG1 were respectively named as $U937^{empty}$ and $U937^{NDRG1}$ cells. After cells were incubated in the tetracycline-free medium for the different days as indicated, $U937^{NDRG1}$ cells expressing NDRG1 were identified by Western blot analysis. $U937^{empty}$ served as a negative control. (B) After grown in medium with or without tetracycline for 6 days, $U937^{empty}$ and $U937^{NDRG1}$ cells were treated with 200 nM NSC606985 for hours as indicated, respectively. The indicated protein levels were detected by Western blots probed with specific antibodies. Symbol Δ represents the cleaved fragment of corresponding protein. Equal loading of protein was confirmed using anti-β-tubulin.

containing medium, in which NDRG1 protein was down-regulated after 12 h, $U937^{NDRG1}$ cells in tetracycline-free medium remained at stable level of NDRG1 protein during NSC606985 treatment (Fig. 5B). When treated with NSC606985 for 24 h, as depicted in Fig. 5B, catalytic fragment of PKCδ was significantly suppressed in $U937^{NDRG1}$ cells grown in tetracycline-free medium compared to $U937^{empty}$ cells. In line with delayed activation of PKCδ, the overexpression of NDRG1 also delayed the cleaved activation of caspase-3 and degradation of its substrate PARP in NSC606985-treated $U937^{NDRG1}$ cells (Fig. 5B). Accordingly, the overexpression of NDRG1 also significantly suppressed 200 nM NSC606985-induced apoptosis in U937 cells, as evidenced by annexin V assay (Figs. 6A and B).

3.5 The suppression of NDRG1 expression by siRNA enhances activation of PKCδ and apoptosis induction

To further validate the role of NDRG1 protein in the activation of PKCδ and apoptosis induction, siRNA specifically targeting NDRG1 mRNA was transfected into the parental

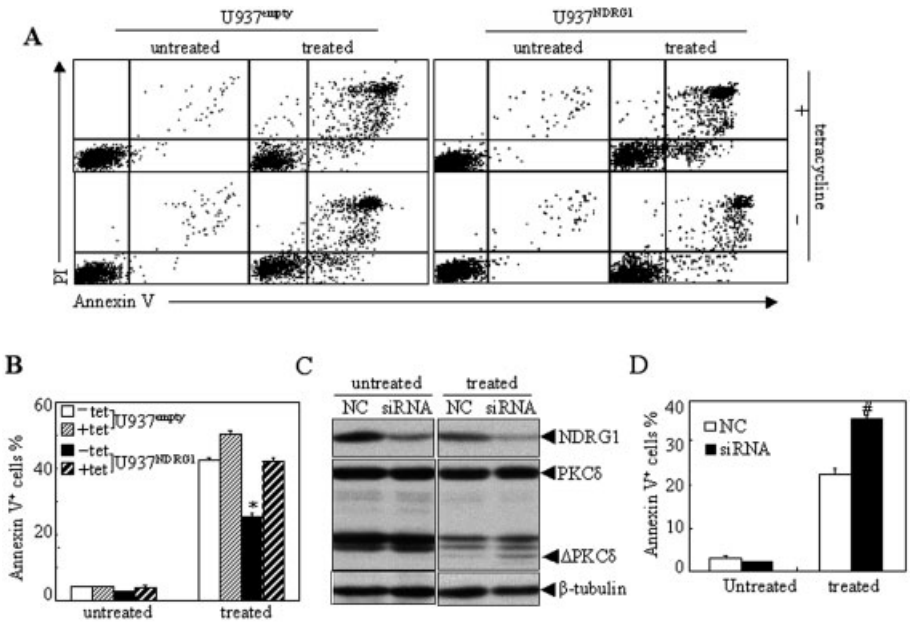

Figure 6. NDRG1 suppresses NSC606985-induced apoptosis. (A, B) U937^{empty} and U937^{NDRG1} cells were grown in medium with or without tetracycline (tet) for 6 days, followed by treatment with or without 200 nM NSC606985 for 36 h (A), and annexin V-positive cells % was determined by flow cytometry (B). The data represent means of three independent experiments with bar as SD. The symbol * represent $p<0.001$ compared with other three column in treated cells. (C, D) U937 cells were stably transfected with specific siRNA against NDRG1 (siRNA) or negative control (NC). Then, these cells were treated with or without 50 nM of NSC606985 overnight. The indicated proteins were detected by Western blots probed with specific antibodies with β-tubulin as equal loading control (C), and annexin V-positive cells % was shown (D). The data represent means of three independent experiments with bar as SD. The symbol # represent $p<0.001$ compared with NC-transfected and NSC606985-treated cells. All experiments were repeated three times with the same results.

U937 cells with negative control siRNA as a control. After selection by G418, the NDRG1-specific siRNA but not the negative control siRNA significantly eliminated NDRG1 expression (Fig. 6C). When treated with 50 nM of NSC606985 for 21 h, the suppression of NDRG1 expression by the specific siRNA significantly enhanced NSC606985-induced activation of PKCδ (Fig. 6C) and apoptosis of U937 cells (Fig. 6D).

4 Discussion

Proteomics has been successfully applied to discover molecules involved in apoptotic cells in a series of studies [26–29]. As an example, with camptothecin analog NSC606985-induced apoptotic U937 cell as model, our laboratory has identified lots of proteins deregulated or translocated among cellular compartments after proteolytic activation of PKCδ and caspase-3 in subcellular proteomics analysis [30]. In this study, to reveal proteins deregulated at early phases of apoptosis, we performed quantitative proteomic analysis of NSC606985-treated leukemic U937 cells at 12 and 18 h, when the PKCδ and caspase-3 are not yet activated. A set of proteins were identified to be significantly deregulated. These involved proteins in cytoskeleton and molecular chaperoning, DNA and RNA processing, glycolysis and energy metabolism, cell proliferation and apoptosis, and other cellular functions. With the aim to find protein that modulates the activation of PKCδ and caspase-3, the proteins that have been documented to be involved in apoptosis warranted further functional analysis. Here, we focused on the down-regulated NDRG1 protein before PKCδ activation during NSC606985-induced apoptosis, and the potential role of other deregulated proteins during apoptosis initiation remain to be explored.

NDRG1 is also known as Drg1, Cap43, RTP/rit42, and Proxy-1 [31–34], which was discovered simultaneously by Van Belzen *et al.* [31] and Kokame *et al.* [35] under differing physiological conditions. It is a member of the new NDRG gene family, which belongs to the α/β hydrolase superfamily, but without presenting a hydrolytic catalytic site. Lachat *et al.* [36] found that NDRG1 is located primarily in the cytoplasm, but it is also associated with the cellular membrane and adherent junctions in a large set of normal human tissues at light- and electron-microscopic levels. The multiple localizations propose the pleiotropic functions of NDRG1. Actually, it was proposed to be involved in cell differentiation, ischemic cell damage, apoptosis, as well as cancer metastasis, which was thought as a new ally in the fight against cancer [36, 37]. In this study, we found that NDRG1 was down-regulated during apoptosis induction at least by DNA-damaging agents such as camptothecin analogue

NSC606985, topotecan and irinoticon treatment. Further, dynamic analysis showed that the down-regulation was an early event prior to the cleavage of PKCδ and activation of caspase-3, and the chemical inhibition of these two enzymes failed to modulate the down-regulation of NDRG1 protein. As summarized by Lachat *et al.* [36], various chemical agents (including synthetic ligands of the PPARγ/RXR transcriptional pathway, androgens, Ni^{2+} compounds, calcium ionophores, okadaic acid) as well as inhibition of DNA methylation and histone deacetylation, activate NDRG1 expression, and diverse physiological and pathological conditions (such as hypoxia, cellular differentiation, N-myc and neoplasia) modulate NDRG1 transcription, mRNA stability, and translation. Meanwhile, NDRG1 is transcriptionally up-regulated in a P53-dependent manner after DNA-damaging agents treatment [22, 33]. However, our results demonstrated that the NDRG1 mRNA was not significantly changed in U937 cells after NSC606985 treatment, which was consistent with the fact that the leukemic U937 cells are bearing mutant inactive P53 [39]. Furthermore, CHX inhibition test showed that the inhibition of new protein synthesis by CHX failed to change the half-life of NDRG1 protein in the presence and absence of NSC606985 treatment, which would suggest that the inhibition of translation was involved in the rapid down-regulation of NDRG1 under the treatment of DNA-damaging agents, although CHX treatment also cleaved PKCδ and induced caspase-3 activation.

To investigate the influence of NDRG1 expression on the proteolytic activation of PKCδ, we generated an inducible NDRG1-expressing cell line using the myeloid leukemic U937 cells. Using this cell line, we demonstrated that inducible NDRG1 expression delayed the cleavage activation of PKCδ in U937 cells. On the contrary, the suppression of NDRG1 expression by specific siRNA significantly enhanced NSC606985-induced activation of PKCδ of U937 cells. These results suggested that the down-regulated NDRG1 might be associated with DNA-damaging agents-induced cleaved activation of PKCδ, although the detailed mechanism of how NDRG1 influences the proteolysis of PKCδ is still under investigation. In consideration of the key role of proteolytic activation of PKCδ in NSC606985-induced leukemic cell apoptosis, we proposed the reduced NDRG1 protein level might also contribute to the leukemic cell apoptosis. As expected, NDRG1 overexpression significantly suppressed NSC606985-induced apoptosis in U937 cells. On the contrary, the suppression of NDRG1 expression by a specific siRNA construct significantly enhanced NSC606985-induced apoptosis of U937 cells. These results indicated that NDRG1 might have an anti-apoptotic role in the AML cells. In accordance to these results, it was documented that tumors established from NDRG1 overexpressing SW620 cells (p53-deficient) were more resistant to CPT-11 as compared with tumors established from vector transfected SW620 cells in mice [38]. However, NDRG1 had been also documented to be necessary for P53-mediated apoptosis [22]. We proposed that the loss or mutation of P53 in those cell lines might contribute the functional diversity of NDRG1 in apoptotic process. There is more than 50% of cancers bearing a mutant impotent P53 or loss of wild type P53. Therefore, the role of NDRG1 in apoptosis should be carefully determined, given that NDRG1 has been marked as a new ally in the fight against cancer in the past years [37].

We thank Dr. P. Liang of Vanderbilt University Medical Center for providing the plasmid pBI-EGFP-NDRG1. This work was supported in part by National Key Technologies R&D Program (No.2006CB910100, 2006AA02Z105), National Key Science Program (NO2009CB918400), National Natural Science Foundation (90813034; 30500215; 30600216), Science and Technology Commission of Shanghai (08JC1413700; 04QMX1467). Dr. G. Q. Chen is a Chang Jiang Scholar of Ministry of Education of China, and is supported by Shanghai Ling-Jun Talent Program. The work is submitted in partial fulfillment of the PhD requirement for Ying Zheng at Shanghai Jiao Tong University School of Medicine.

The authors have declared no conflict of interest.

5 References

[1] Raff, M. C., Social controls on cell survival and cell death. *Nature* 1992, *356*, 397–400.

[2] Vermeulen, K., Van Bockstaele, D. R., Berneman, Z. N., Apoptosis: mechanisms and relevance in cancer. *Ann. Hematol.* 2005, *84*, 627–639.

[3] Havelka, A. M., Berndtsson, M., Olofsson, M. H., Shoshan, M. C., Linder, S., Mechanisms of action of DNA-damaging anticancer drugs in treatment of carcinomas: is acute apoptosis an "off-target" effect? *Mini Rev. Med. Chem.* 2007, *7*, 1035–1039.

[4] Riedl, S. J., Shi, Y., Molecular mechanisms of caspase regulation during apoptosis. *Nat. Rev. Mol. Cell. Biol.* 2004, *5*, 897–907.

[5] Nunez, G., Benedict, M. A., Hu, Y., Inohara, N., Caspases: the proteases of the apoptotic pathway. *Oncogene* 1998, *17*, 3237–3245.

[6] Livneh, E., Fishman, D. D., Linking protein kinase C to cell-cycle control. *Eur. J. Biochem.* 1997, *248*, 1–9.

[7] Watanabe, T., Ono, Y., Taniyama, Y., Hazama, K. *et al.*, Cell division arrest induced by phorbol ester in CHO cells overexpressing protein kinase C-delta subspecies. *Proc. Natl. Acad. Sci. USA* 1992, *89*, 10159–10163.

[8] Emoto, Y., Manome, Y., Meinhardt, G., Kisaki, H. *et al.*, Proteolytic activation of protein kinase C delta by an ICE-like protease in apoptotic cells. *EMBO J.* 1995, *14*, 6148–6156.

[9] Mizuno, K., Noda, K., Araki, T., Imaoka, T. *et al.*, The proteolytic cleavage of protein kinase C isotypes, which generates kinase and regulatory fragments, correlates with Fas-mediated and 12-O-tetradecanoyl-phorbol-13-acetate-induced apoptosis. *Eur. J. Biochem.* 1997, *250*, 7–18.

[10] Denning, M. F., Wang, Y., Nickoloff, B. J., Wrone-Smith, T., Protein kinase C delta is activated by caspase-dependent

proteolysis during ultraviolet radiation-induced apoptosis of human keratinocytes. *J. Biol. Chem.* 1998, *273*, 29995–30002.

[11] Reyland, M. E., Anderson, S. M., Matassa, A. A., Barzen, K. A., Quissell, D. O., Protein kinase C delta is essential for etoposide-induced apoptosis in salivary gland acinar cells. *J. Biol. Chem.* 1999, *274*, 19115–19123.

[12] Basu, A., Woolard, M. D., Johnson, C. L., Involvement of protein kinase C delta in DNA damage-induced apoptosis. *Cell Death Differ.* 2001, *8*, 899–908.

[13] Yoshida, K., PKCdelta signaling: mechanisms of DNA damage response and apoptosis. *Cell. Signal.* 2007, *19*, 892–901.

[14] Basu, A., Akkaraju, G. R., Regulation of caspase activation and cis-diamminedichloroplatinum(II)-induced cell death by protein kinase C. *Biochemistry* 1999, *38*, 4245–4251.

[15] Song, M. G., Gao, S. M., Du, K. M., Xu, M. *et al.*, Nanomolar concentration of NSC606985, a camptothecin analog, induces leukemic-cell apoptosis through protein kinase C delta-dependent mechanisms. *Blood* 2005, *105*, 3714–3721.

[16] Leverrier, S., Vallentin, A., Joubert, D., Positive feedback of protein kinase C proteolytic activation during apoptosis. *Biochem. J.* 2002, *368*, 905–913.

[17] Blass, M., Kronfeld, I., Kazimirsky, G., Blumberg, P. M., Brodie, C., Tyrosine phosphorylation of protein kinase C delta is essential for its apoptotic effect in response to etoposide. *Mol. Cell. Biol.* 2002, *22*, 182–195.

[18] Anantharam, V., Kitazawa, M., Wagner, J., Kaul, S., Kanthasamy, A. G., Caspase-3-dependent proteolytic cleavage of protein kinase C delta is essential for oxidative stress-mediated dopaminergic cell death after exposure to methylcyclopentadienyl manganese tricarbonyl. *J. Neurosci.* 2002, *22*, 1738–1751.

[19] Tonge, R., Shaw, J., Middleton, B., Rowlinson, R. *et al.*, Validation and development of fluorescence two-dimensional differential gel electrophoresis proteomics technology. *Proteomics* 2001, *1*, 377–396.

[20] Han, Y. H., Xia, L., Song, L. P., Zheng, Y. *et al.*, Comparative proteomic analysis of hypoxia-treated and untreated human leukemic U937 cells. *Proteomics* 2006, *6*, 3262–3274.

[21] Boer, J., Bonten-Surtel, J., Grosveld, G., Overexpression of the nucleoporin CAN/NUP214 induces growth arrest, nucleocytoplasmic transport defects, and apoptosis. *Mol. Cell. Biol.* 1998, *18*, 1236–1247.

[22] Stein, S., Thomas, E. K., Herzog, B., Westfall, M. D. *et al.*, NDRG1 is necessary for p53-dependent apoptosis. *J. Biol. Chem.* 2004, *279*, 48930–48940.

[23] Chen, B., Nelson, D. M., Sadovsky, Y., N-myc down-regulated gene 1 modulates the response of term human trophoblasts to hypoxic injury. *J. Biol. Chem.* 2006, *281*, 2764–2772.

[24] Zhao, K. W., Li, X., Zhao, Q., Huang, Y. *et al.*, Protein kinase C delta mediates retinoic acid and phorbol myristate acetate-induced phospholipid scramblase 1 gene expression: its role in leukemic cell differentiation. *Blood* 2004, *104*, 3731–3738.

[25] Yan, H., Wang, Y. C., Li, D., Wang, Y. *et al.*, Arsenic trioxide and proteasome inhibitor bortezomib synergistically induce apoptosis in leukemic cells: the role of protein kinase C delta. *Leukemia* 2007, *21*, 1488–1495.

[26] Carie, A. E., Sebti, S. M., A chemical biology approach identifies a beta-2 adrenergic receptor agonist that causes human tumor regression by blocking the Raf-1/Mek-1/Erk1/2 pathway. *Oncogene* 2007.

[27] Huang, Z., The chemical biology of apoptosis. Exploring protein-protein interactions and the life and death of cells with small molecules. *Chem. Biol.* 2002, *9*, 1059–1072.

[28] Thiede, B., Rudel, T., Proteome analysis of apoptotic cells. *Mass Spectrom. Rev.* 2004, *23*, 333–349.

[29] Machuy, N., Thiede, B., Rajalingam, K., Dimmler, C. *et al.*, A global approach combining proteome analysis and phenotypic screening with RNA interference yields novel apoptosis regulators. *Mol. Cell. Proteomics* 2005, *4*, 44–55.

[30] Yu, Y., Wang, L. S., Shen, S. M., Xia, L. *et al.*, Subcellular proteome analysis of camptothecin analogue NSC606985-treated acute myeloid leukemic cells. *J. Proteome Res.* 2007, *6*, 3808–3818.

[31] van Belzen, N., Dinjens, W. N., Diesveld, M. P., Groen, N. A. *et al.*, A novel gene which is up-regulated during colon epithelial cell differentiation and down-regulated in colorectal neoplasms. *Lab. Invest.* 1997, *77*, 85–92.

[32] Zhou, D., Salnikow, K., Costa, M., Cap43, a novel gene specifically induced by Ni2+ compounds. *Cancer Res.* 1998, *58*, 2182–2189.

[33] Kurdistani, S. K., Arizti, P., Reimer, C. L., Sugrue, M. M. *et al.*, Inhibition of tumor cell growth by RTP/rit42 and its responsiveness to p53 and DNA damage. *Cancer Res.* 1998, *58*, 4439–4444.

[34] Park, H., Adams, M. A., Lachat, P., Bosman, F. *et al.*, Hypoxia induces the expression of a 43-kDa protein (PROXY-1) in normal and malignant cells. *Biochem. Biophys. Res. Commun.* 2000, *276*, 321–328.

[35] Kokame, K., Kato, H., Miyata, T., Homocysteine-respondent genes in vascular endothelial cells identified by differential display analysis. GRP78/BiP and novel genes. *J. Biol. Chem.* 1996, *271*, 29659–29665.

[36] Lachat, P., Shaw, P., Gebhard, S., van Belzen, N. *et al.*, Expression of NDRG1, a differentiation-related gene, in human tissues. *Histochem. Cell. Biol.* 2002, *118*, 399–408.

[37] Kovacevic, Z., Richardson, D. R., The metastasis suppressor, Ndrg-1: a new ally in the fight against cancer. *Carcinogenesis* 2006, *27*, 2355–2366.

[38] Motwani, M., Sirotnak, F. M., She, Y., Commes, T., Schwartz, G. K., Drg1, a novel target for modulating sensitivity to CPT-11 in colon cancer cells. *Cancer Res.* 2002, *62*, 3950–3955.

[39] Shiohara, M., Akashi, M., Gombart, A. F., Yang, R., Koeffler, H. P., Tumor necrosis factor alpha: posttranscriptional stabilization of WAF1 mRNA in p53-deficient human leukemic cells. *J. Cell. Physiol.* 1996, *166*, 568–576.

